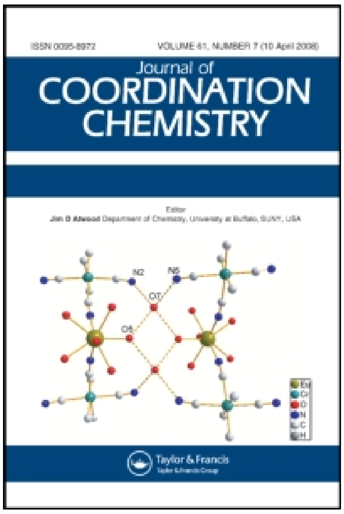

Journal of Coordination Chemistry
Publication details, including instructions for authors and subscription information:
http://www.informaworld.com/smpp/title~content=t713455674

Two organic-inorganic hybrids based on polyoxometalates: synthesis, crystal structure, and characterization

Feng Yao[a]; Fan-Xia Meng[ab]; Ya-Guang Chen[a]; Chun-Jing Zhang[a]
[a] Key Laboratory of Polyoxometalates Science of Ministry of Education, College of Chemistry, Northeast Normal University, Changchun 130024, P. R. China [b] First High School of Ji-An, Ji-An 133000, Jilin Province, P. R. China

First published on: 28 October 2009

To cite this Article Yao, Feng , Meng, Fan-Xia , Chen, Ya-Guang and Zhang, Chun-Jing(2010) 'Two organic-inorganic hybrids based on polyoxometalates: synthesis, crystal structure, and characterization', Journal of Coordination Chemistry, 63: 2, 196 — 205, First published on: 28 October 2009 (iFirst)

To link to this Article: DOI: 10.1080/00958970903377287

URL: http://dx.doi.org/10.1080/00958970903377287

Journal of Coordination Chemistry
Vol. 63, No. 2, 20 January 2010, 196–205

Taylor & Francis
Taylor & Francis Group

Two organic–inorganic hybrids based on polyoxometalates: synthesis, crystal structure, and characterization

FENG YAO†, FAN-XIA MENG†‡, YA-GUANG CHEN*† and
CHUN-JING ZHANG†

†Key Laboratory of Polyoxometalates Science of Ministry of Education, College of
Chemistry, Northeast Normal University, Changchun 130024, P. R. China
‡First High School of Ji-An, Ji-An 133000, Jilin Province, P. R. China

(*Received 23 June 2009; in final form 29 July 2009*)

Two new Keggin- and Wells-Dawson-type polyoxometalate-based organic–inorganic hybrid copper–organonitrogen complexes have been synthesized under hydrothermal conditions: $[Cu^{I}(4,4'\text{-bpy})]_2[H_2SiW_{12}O_{40}]\cdot 2H_2O$ (4,4′-bpy = 4,4′-bipyridine) (**1**) and $\{[Cu^{I}(4,4'\text{-bpy})]_3[Cu^{II}(en)_2]_2[As_2W^{V}_3W^{VI}_{15}O_{62}]\}_2[Cu^{I}_3(4,4'\text{-bpy})_3(H_2O)_2](H_3O)\cdot 4H_2O$ (**2**) (en = ethylenediamine), and characterized by elemental analysis, IR spectra, TGA, XRD, and single crystal X-ray diffraction. In **1**, $[Cu(4,4'\text{-bpy})]^+$ cations form polymeric chains $[Cu(4,4'\text{-bpy})]_n^{n+}$ and a weak Cu–O linkage makes the anions situate between two chains, forming an infinite 1-D ladder-chain structure. Such 1-D ladder-chains are further interconnected *via* hydrogen bonding into a 3-D supramolecular framework. Compound **2** with covalently bonded 3-D structure consists of saturated Wells-Dawson tungstoarsenate polyoxoanions and copper complexes with two types (rigid and flexible) of ligands. The polyoxoanion has the highest connectivity for Wells-Dawson tungstoarsenate polyoxoanion coordination polymers to date. XPS spectra indicate that three W atoms in the Dawson unit were reduced and that there coexist Cu^{I} and Cu^{II} in **2**.

Keywords: Polyoxometalates; Keggin; Wells-Dawson; Tungstoarsenate; Organic–inorganic hybrids

1. Introduction

Polyoxometalates (POMs) [1], an important family of metal–oxygen cluster species, hold a prominent position owing to their intriguing architectures and potential applications in catalysis, photochemistry, magnetism, and medicine [2]. Recent effort has been devoted to the decoration of well-known POMs with various transition metal complexes (TMCs) [3–7] in order to obtain organic–inorganic hybrids that combine pronounced structural diversity [8, 9] and potential applications in catalysis [10], new functional materials [11], and biochemistry [12], etc., which enriches significantly the chemistry of POM-based hybrids. In the course of our investigations of the hydrothermal synthesis of POM-based hybrid materials, 1-D, 2-D, and 3-D materials

---

*Corresponding author. Email: chenyg146@nenu.edu.cn

Journal of Coordination Chemistry
ISSN 0095-8972 print/ISSN 1029-0389 online
DOI: 10.1080/00958970903377287

can be constructed from the common Keggin, Wells-Dawson clusters and Cu–organonitrogen complexes.

Keggin polyoxoanions are an ideal inorganic building block for the construction of inorganic–organic hybrid materials due to their diverse coordination styles through terminal and bridging oxygens and suitable size. There are some reports about inorganic–organic hybrids based on Keggin anions [13–23]. On the other hand, compared with Keggin polyoxoanion, Wells-Dawson polyoxoanion with 18 terminal O atoms and 36 μ_2-O atoms can offer more coordination sites to link metal–organic units, but their large size decreases the electron density and the oxygen coordination ability on their surfaces at the same time [24]. One strategy has been exploited to increase the surface charge density and to activate the surface oxygens of polyoxoanions by decreasing the oxidation states of metal centers in POMs, for example, from $W(Mo)^{VI}$ to $W(Mo)^{V}$, with reducing reagents [25]. In contrast to common Wells-Dawson tungstoarsenate polyoxoanion, reduced Wells-Dawson tungstoarsenate polyoxoanion has more negative charges which should be excellent precursors for constructing the high-dimensional materials. Although several 3-D POM coordination polymers based on Wells-Dawson tungstophosphates have been reported by Peng's group [26, 27], 3-D derivatives based on Wells–Dawson tungstoarsenate have not been reported hitherto.

In our work we choose the rigid 4,4′-bipyridine (4,4′-bpy) and flexible ethylenediamine (en) ligands and $Cu(Ac)_2$ to construct multidimensional organic–inorganic hybrids due to: (1) the linear rigid ligand, 4,4′-bpy, contains two terminal pyridyl groups in opposite positions, which is helpful to construct high-dimensional structures; (2) chelating flexible ligand, en, not only makes the coordination of transition metal diverse, but also stabilizes transition metal complexes by chelating; (3) Cu has changeable oxidation states and 4s, 4p, 4d vacant orbits, as well as easily deformed $3d^9/3d^{10}$ electronic clouds, all of which make it readily accept solitary electronic pairs from ligands. Fortunately, using Keggin and Wells-Dawson polyoxoanions as inorganic building blocks, we have synthesized **1** with 1-D bitrack chains based on Keggin POM, $[Cu^{I}(4,4'\text{-bpy})]_2[H_2SiW_{12}O_{40}]\cdot 3H_2O$, very different from reported compounds [22, 23] in its structure, and **2** with covalently bonded 3-D framework based on the Wells-Dawson POM, $\{[Cu^{I}(4,4'\text{-bpy})]_3[Cu^{II}(en)_2]_2[As_2W^{V}_{3}W^{VI}_{15}O_{62}]\}_2[Cu^{I}_{3}(4,4'\text{-bpy})_3(H_2O)_2](H_3O)\cdot 4H_2O$ (**2**).

2. Experimental

2.1. *Materials and general methods*

All reagents were commercially available and used without purification. Elemental analyses (C, H, and N) were performed on a Perkin-Elmer 2400 CHN Elemental Analyzer, W and Cu were determined by a Leaman inductively coupled plasma spectrometer. IR spectra on KBr pellets were recorded on a Nicolet 170SX FT-IR spectrophotometer from 400 to 4000 cm^{-1}. XPS analyses were performed on a VGESCALABMK spectrometer with a Mg-Kα (1253.6 eV) achromatic X-ray source. EPR spectra were recorded on a JESFE3AX spectrometer at room temperature. TG analyses were recorded with a Netzsch STA 449C microanalyzer in an atmosphere of nitrogen at a heating rate of $10^{\circ}C\,min^{-1}$.

2.2. *Hydrothermal synthesis*

2.2.1. Synthesis of $[Cu^I(4,4'\text{-bpy})]_2[H_2SiW_{12}O_{40}] \cdot 3H_2O$ (1). $H_4SiW_{12}O_{40} \cdot 18H_2O$ [28] (1.15 g, 0.356 mmol), $Cu(Ac)_2 \cdot 2H_2O$ (0.16 g, 0.7 mmol), 4,4′-bipy (0.05 g, 0.32 mmol), and en (0.25 g, 4.16 mmol) were dissolved in 10 mL water. The pH of the resulting mixture was adjusted to 2.7 by adding HCl solution, and then the mixture was stirred for 30 min in air. The final solution was transferred into a 25 mL Teflon-lined autoclave at 170°C for 3 days. Then the autoclave was cooled at $10°C\,h^{-1}$ to room temperature. The resulting dark red block crystals were filtered off, washed with distilled water, and dried in a desiccator at room temperature (38% yield based on W). Calcd for $C_{20}H_{24}N_4Cu_2O_{43}SiW_{12}$ (3369.79) (%): C, 7.13; H, 0.72; N, 1.66; Cu, 3.77; W, 65.47). Found (%): C, 6.92; H, 0.65; N, 1.64; Cu, 3.64; W, 65.89. IR (KBr pellet (cm^{-1})): 3436 (s), 3088 (w), 1610 (m), 1482 (s), 1401 (m), 1368 (w), 1232 (m), 1208 (m), 975 (s), 921 (s), 881 (s), 793 (s), 523 (m).

2.2.2. Synthesis of $\{[Cu^I(4,4'\text{-bpy})]_3[Cu^{II}(en)_2]_2[As_2W^V_3W^{VI}_{15}O_{62}]\}_2[Cu^I_3(4,4'\text{-bpy})_3(H_2O)_2](H_3O) \cdot 4H_2O$ (2). $K_6As_2W_{18}O_{62} \cdot 14H_2O$ [29] (1.48 g, 0.3 mmol), $Cu(Ac)_2 \cdot 2H_2O$ (0.16 g, 0.7 mmol), 4,4′-bipy (0.05 g, 0.32 mmol), en (0.1 g, 1.66 mmol), and Et_3N (0.3 mL) were dissolved in 10 mL water. The pH of the mixture was adjusted to 4.4 by adding HCl solution and the mixture was stirred for 30 min in air. The final solution was transferred into a 25 mL Teflon-lined autoclave and crystallized at 170°C for 5 days. Then the autoclave was cooled at $10°C\,h^{-1}$ to room temperature. The resulting black block crystals were filtered off, washed with distilled water, and dried in a desiccator at room temperature (35% yield based on W). Calcd for $C_{53}H_{75}N_{17}Cu_{6.5}O_{65.5}As_2W_{18}$ (5870.45) (%): C, 10.84; H, 1.29; N, 4.06; Cu, 7.04; W, 56.37. Found (%): C, 10.93; H, 1.35; N, 3.98; Cu, 6.88; W, 56.12. IR (KBr pellet (cm^{-1})): 3437 (s), 3079 (w), 2951 (w), 2868 (w), 1604 (m), 1488 (s), 1406 (m), 1362 (w), 1238 (m), 1202 (m), 954 (s), 864 (s), 831 (s), 735 (s), 521 (m).

2.3. *X-ray crystallography*

The single-crystal X-ray diffraction data of **1** and **2** were collected on a Siemens Smart CCD diffractometer at 293 K using graphite-monochromated Mo-Kα radiation ($\lambda = 0.71073$ Å) and omega scans technique. Empirical absorption correction was applied. The structures of **1** and **2** were solved by direct methods and refined by full-matrix least-squares on F^2 using SHELXL 97 software [30]. The positions of the hydrogen attached to carbon were fixed according to riding mode. A summary of crystallographic data and structural determinations for **1** and **2** is provided in table 1.

3. Results and discussion

3.1. *Hydrothermal synthesis*

Isolations of **1** and **2** depend on the exploitation of hydrothermal technique [31]. In a specific hydrothermal process, many factors can affect the formation and crystal growth

Table 1. Crystallographic data and structure refinement for **1** and **2**.

Compound	**1**	**2**
Empirical formula	$C_{20}H_{22}Cu_2N_4O_{42}SiW_{12}$	$C_{53}H_{75}As_2Cu_{6.5}N_{17}O_{69}W_{18}$
Formula weight	3351.77	5870.45
Crystal system	Triclinic	Triclinic
Space group	$P\bar{1}$	$P\bar{1}$
Unit cell dimensions (Å, °)		
a	10.8597(5)	13.249(5)
b	11.8517(6)	17.813(5)
c	13.3478(10)	23.940(5)
α	104.250	82.266(5)
β	103.253	78.135(5)
γ	114.883	83.648(5)
Volume (Å^3), Z	1398.11(14), 1	5459(3), 2
Calculated density (g cm^{-3})	4.088	3.566
Absorption coefficient (mm^{-1})	25.445	20.811
$F(000)$	1508	5229
Crystal size (mm^3)	0.129 × 0.117 × 0.108	0.155 × 0.110 × 0.100
θ range for data collection (°)	1.70–26.00	1.16–27.29
Limiting indices	$-13 \le h \le 6$; $-13 \le k \le 14$; $-16 \le l \le 16$	$-17 \le h \le 16$; $-22 \le k \le 20$; $-30 \le l \le 25$
Data/restraints/parameters	5385/0/394	24,523/0/1377
Goodness of fit on F^2	1.019	0.939
Final R indices [$I > 2\sigma(I)$]	$R_1 = 0.0472$, $wR_2 = 0.1283$	$R_1 = 0.0608$, $wR_2 = 0.1631$
Final indices (all data)	$R_1 = 0.0538$, $wR_2 = 0.1335$	$R_1 = 0.1043$, $wR_2 = 0.1923$

$R_1 = \sum \|F_o|-|F_c\|/\sum |F_o|$; $wR_2 = \sum\left[w(F_o^2 - F_c^2)^2\right]/\sum\left[w(F_o^2)^2\right]^{1/2}$.

of products, such as the type and ratio of initial reactants, starting concentration, pH, reaction time, and temperature. There are several reports about SiW_{12}-Cu-4,4′-bipy compounds [32–37]. Only one of the initial reactants in these reports [33, 38] and our experiments is different; the products have obviously different structures from 1-D to 3-D in very similar hydrothermal conditions. Peng [34, 35] and Zheng [36] reported 2-D and 3-D polymers using $CuCl_2$ and $Cu(NO_3)_2$ as initial materials and Et_3N.

In our case, under the presence of en which may act as a reductant and did not appear in the product, we obtained a 1-D ladder-chain compound **1** using $H_4SiW_{12}O_{40} \cdot 18H_2O$, $Cu(Ac)_2 \cdot 2H_2O$ and 4,4′-bpy. Our parallel experiments and the literature [33, 35] show that the pH of the reaction system is crucial for the crystallization of hybrids. Crystals of **1** and **2** could only be obtained at pH 2.6 and 4.4, respectively. With identical conditions except the pH (4.2–6.2) of reaction solution and absence of en, we have obtained SiW_{12}-Cu-4,4′-bipy products with 3-D structure [37]. The nature of the divalent transition-metal is crucial for the formation of **1** and **2**. We tried to replace $Cu(Ac)_2 \cdot 2H_2O$ with $Co(Ac)_2 \cdot 4H_2O$ or $Ni(Ac)_2 \cdot 4H_2O$, but no isostructural compounds were obtained. Compared with **1**, addition of Et_3N in the synthesis of **2** leads to the separation of **2** with 3-D framework. So it can be deduced that Et_3N played an important role in the dimensionality of **1** and **2**. References [34] and [35] show the same phenomena.

3.2. *Description of the structures*

Single-crystal X-ray diffraction analysis reveals that **1** is composed of one $[\alpha\text{-}SiW_{12}O_{40}]^{4-}$, two [Cu(4,4′-bpy)] units, and three lattice H_2O, as shown in figure 1.

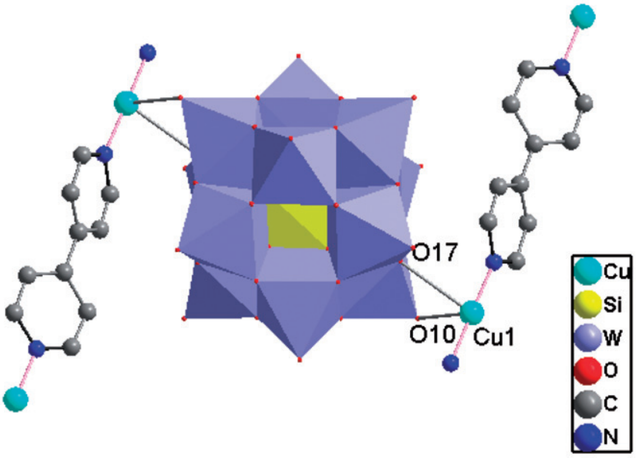

Figure 1. Polyhedral representation of **1**; atoms are labeled, hydrogen atoms and water molecules are omitted for clarity.

In the $[\alpha\text{-SiW}_{12}O_{40}]^{4-}$ anion, the oxygens can be divided into four groups: O_a (connecting the Si heteroatom and W atoms), O_c (shared by two WO_6 octahedra in the same W_3O_{13} unit), O_b (connecting two W_3O_{13} units), and O_t (terminal connecting only one W); relevant W–O bonds can be grouped into three groups: W–O_t bonds, W–$O_{b,c}$ bonds, and W–O_a bonds, whose bond distances fall in the ranges of 1.668(11)–1.689(9) Å, 1.872(14)–1.927(15) Å, and 2.330(15)–2.455(17) Å with averages of 1.679, 1.895, and 2.402 Å, respectively. The mean values of the W–O_t and W–$O_{b/c}$ are shorter than in the literature [39], and the mean value of W–O_a is longer in the literature [39]. These results show that WO_6 octahedra of the polyoxoanion are distorted due to influence of the outer coordination environment and verify the existence of the interactions between the polyoxoanions $[\alpha\text{-SiW}_{12}O_{40}]^{4-}$ and copper and hydrogen bond interaction. The central Si of $[\alpha\text{-SiW}_{12}O_{40}]^{4-}$ is surrounded by a cube of eight oxygens with each site half-occupied, common in polyoxometalate chemistry.

In **1** Cu1 is coordinated by two nitrogens from two 4,4′-bpy molecules, forming a metal–organo chain with Cu–N distances of 1.899(14) Å and 1.921(15) Å as well as a N–Cu–N angle of 174.4(7)°. Additionally, Cu1 has weak interactions with O10 and O17 oxygens of the Keggin anion; distances of Cu1–O10 and Cu1–O17 are 2.646(12) Å and 2.743(14) Å, respectively. The weak Cu–O linkage makes the anions situate between two metal–organo chains, forming into a 1-D ladder chain-like structure as shown in figure S1. There exist C–H···O hydrogen bond interactions between terminal oxygens (O5) of the Keggin units of one chain and C4–H4 of an adjacent parallel chain with a O5···H4 distance of 2.602 Å, resulting in the formation of a 2-D layer structure (figure 2). The layers connect *via* C–H···O hydrogen bonds between the bpy molecules and the surface oxygens of the Keggin units in other layers to yield a 3-D architecture; typical hydrogen bonds are O8···H7–C7 and O8···H9–C9 with the O···H distances of 2.680 and 2.602 Å (figure S2). The C–H···O hydrogen bonds play an important role in the architecture of **1**.

Structural analysis of **2** indicates that an asymmetric unit of **2** is composed of two Cu–N polymeric chain cations $[\text{Cu}^{I}(4,4'\text{-bpy})]_3^{3+}$ and $[\text{Cu}^{I}_{1.5}(4,4'\text{-bpy})_{1.5}(H_2O)]^{1.5+}$, two

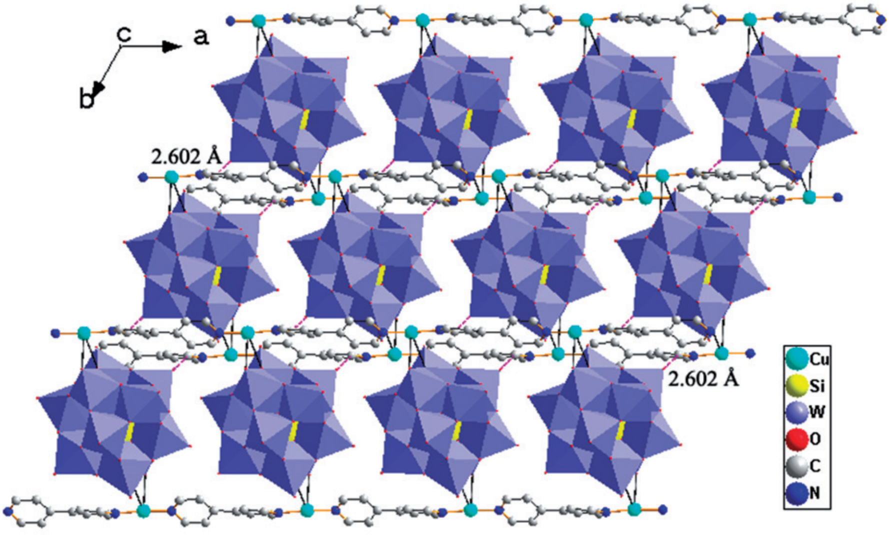

Figure 2. 2-D layer structure of **1** linked by H-bonds on the *ab* plane. Hydrogen atoms and water molecules are omitted for clarity.

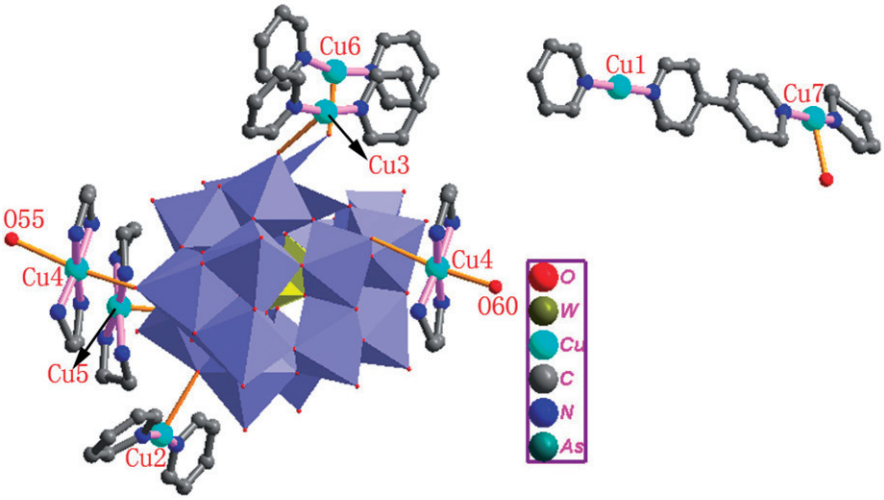

Figure 3. Ball–stick and polyhedral view of the asymmetric unit of **2** and the coordination sites of the As_2W_{18} polyoxoanion. The hydrogen atoms and crystallization water molecules are omitted for clarity.

$[Cu^{II}(en)_2]^{2+}$ cation fragments, one $[As_2W^{V}_{3}W^{VI}_{15}O_{62}]^{9-}$ polyoxoanion and 2.5 lattice water molecules (figure 3). The $[As_2W^{V}_{3}W^{VI}_{15}O_{62}]^{9-}$ polyoxoanion has a classical Wells-Dawson structure [40] and point group symmetry D_{3h}. The W's are divided into two structurally distinct types: six "polar" and 12 "equatorial". It also contains three types of oxygens: eight center oxygens, 36 bridge oxygens, and 18 terminal oxygens, which make the polyoxoanion to have strong coordination ability.

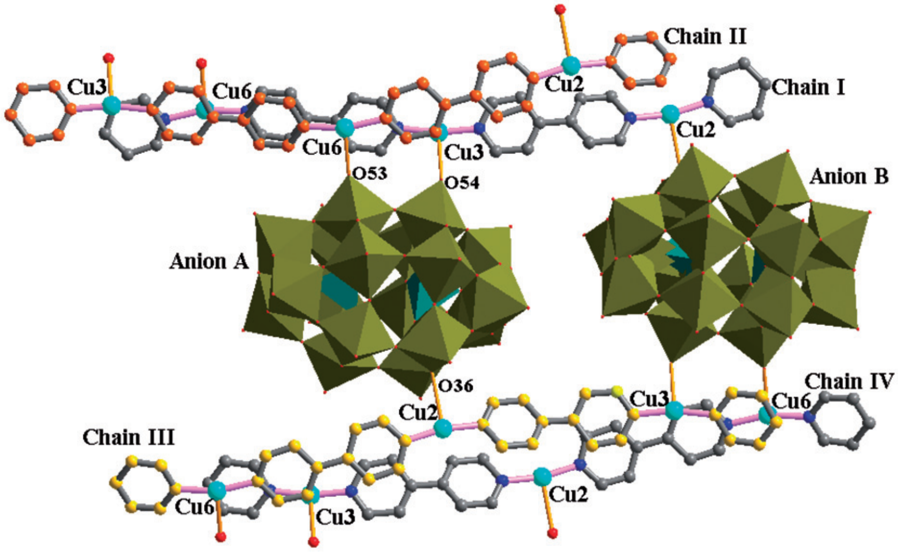

Figure 4. Polyhedral and ball–stick representation of the linkage between Dawson anions and $[Cu^I(4,4'\text{-bpy})]_3^{3+}$ polymer chains. The other parts of **2** are omitted for clarity.

In the asymmetric unit, there are 6.5 crystallographically unique Cu's exhibiting four different coordination environments. Cu1 displays a linear N–Cu–N coordination geometry with Cu–N distance of 1.910(16) Å and N–Cu–N angle of 180.0(8)°. Cu2, Cu3, and Cu6 are three-coordinated with a T-shape geometry, defined by two nitrogens from two 4,4′-bpy ($d_{Cu–N}$, 1.894(16), 1.927(17) Å for Cu2, 1.899(15), 1.893(18) Å for Cu3, 1.928(14), 1.946(15) Å for Cu6) and a terminal oxygen ($d_{Cu2–O36}$, 2.666 Å, $d_{Cu3–O54}$, 2.510 Å, and $d_{Cu6–O53}$, 2.293 Å) from $[As_2W_3^VW_{15}^{VI}O_{62}]^{9-}$. The coordination geometry of Cu7 is similar to that of Cu2, Cu3, and Cu6, except that its coordinated oxygen comes from water with a Cu7–O66 distance of 2.371 Å. The Cu4 is a six-coordinate distorted octahedral configuration built of four nitrogens from two en ligands and two terminal oxygens from two $[As_2W_3^VW_{15}^{VI}O_{62}]^{9-}$ polyoxoanions with axial Cu4–O60 and Cu4-O55′ distances of 2.369 Å and 2.620 Å and equatorial Cu–N distances of 1.951(18)–2.063(17) Å. The distorted octahedral configuration is ascribed to Jahn–Teller effects. Cu5 is a five-coordinate square pyramid defined by four nitrogens ($d_{Cu–N}$, 2.000(17)–2.038(18) Å) from two en ligands and one oxygen from $[As_2W_3^VW_{15}^{VI}O_{62}]^{9-}$ with Cu5–O51 distance of 2.538 Å.

Each copper plays a different role in the construction of 3-D architecture. The 4,4′-bpy molecules serve as bidentate bridging ligands linking Cu2 and Cu6, Cu6 and Cu3, Cu3, and Cu2′, as well as Cu1 and Cu7, forming two types of 1-D $Cu^I(4,4'\text{-bpy})$ complex chains. In the Cu2–Cu6–Cu3 chain, Cu2 and Cu3 ions are coordinated by polyoxoanions on one side of the chain and Cu6 is coordinated by polyoxoanions on the other side of the chain (figure 4). A couple of $[As_2W_3^VW_{15}^{VI}O_{62}]^{9-}$ polyoxoanions in an –A–B–A–B– pattern coordinate to four $Cu^I(4,4'\text{-bpy})$ chains through its outer oxygens. Types A (pink-colored) and B (green-colored) can coincide after 180° of rotation. The A type $[As_2W_3^VW_{15}^{VI}O_{62}]^{9-}$ polyoxoanion links Cu3 belonging to chain I and Cu6 ion belonging to chain II with its two adjacent terminal oxygens and links Cu2

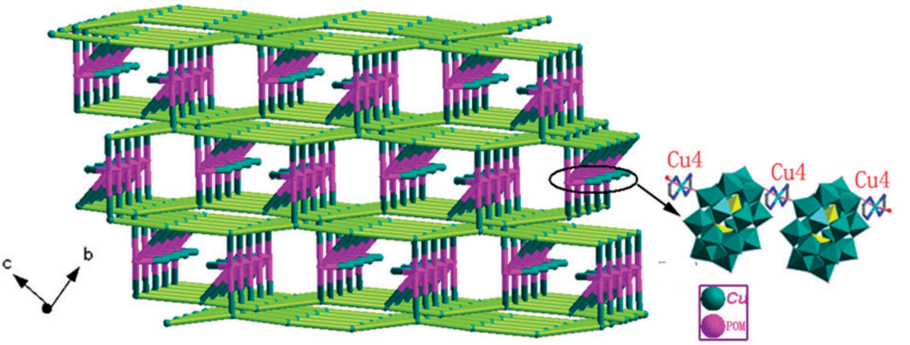

Figure 5. Schematic view of the $[6^2{\cdot}8]^2[8^2{\cdot}10][6^2{\cdot}8^2{\cdot}10^4{\cdot}14^2]$ topology of the 3-D network of **2**. The Wells-Dawson tungstoarsenate polyoxoanions are replaced by pink nodes of the net, green represent Cu ions.

belonging to chain III with its bridging oxygen on the opposite side of the terminal oxygens. The B type $[As_2W^V_3W^{VI}_{15}O_{62}]^{9-}$ polyoxoanion links Cu3 belonging to chain III and Cu6 belonging to chain IV with its two adjacent terminal oxygens and links Cu2 belonging to chain I with its bridging oxygen on the opposite side of the terminal oxygen. As a result, a 2-D layer is formed on the $(1\ 0\ \bar{1})$ plane (figures S3 and S4). Furthermore, Cu4 in $[Cu(en)_2]^{2+}$ is coordinated by O60 of the polyoxoanion in one layer and O55′ belonging to the other layer, which fuses adjacent layers into a 3-D architecture. For the sake of clarity, the 3-D architecture is shown in topology representation $[6^2{\cdot}8]^2[8^2{\cdot}10][6^2{\cdot}8^2{\cdot}10^4{\cdot}14^2]$ (figure 5). In this simplification, the two-connected node is Cu4, three-connected nodes are Cu2, Cu3, and Cu6, and five-connected ones are $[As_2W^V_3W^{VI}_{15}O_{62}]^{9-}$. The Cu1–Cu7 chains in which the Cu ions do not link with POM building blocks act as counter ions and extend parallel to the Cu2–Cu3–Cu6 chains.

EPR spectra for **1** recorded at room temperature (298 K) on crystalline samples shows no signals, indicating no Cu^{II} and W^V in **1**, that is, tungstens are +6 and Cu is +1 in **1**. The oxidation states of W and Cu in **2** are confirmed by XPS measurements, which were performed in the energy regions of W_{4f} and Cu_{2p}, respectively. The XPS spectrum in the energy regions of W_{4f} (figure S5) gives three peaks at 35.113, 37.272, and 39.454 eV, attributable to $W_{4f7/2}$ and $W_{4f5/2}$, respectively. The deconvoluted spectrum gives an area ratio of 3 : 15 for the peaks at 35.113 and 37.27 eV, corresponding to the ratio of W^V and W^{VI} [41]. BVS calculations [42] on W indicate the site occupancy disorder of W^V atoms in As_2W_{18}. The spectrum (figure S6) in the Cu_{2p} region with a peak at 933.9 eV is ascribed to Cu^I, and the satellite peak (943.4 eV) can be used as a fingerprint for identifying the presence of Cu^{II} [43, 44].

3.3. *Thermal analysis*

The TG curve of **1** (figure S7) exhibits two continuous stages of weight loss from 43°C to 619°C corresponding to the release of all water molecules and 4,4′-bpy. The whole weight loss (11.16%) is in good agreement with the calculated value (10.93%). In TG curve of **2** (figure S8), the first weight loss of 1.66% from 43°C to 158°C corresponds to the removal of water (the calculated value for 3.5 water molecules is 1.07%). This weight difference explains that there exist some disordered water molecules in the crystals. At 280°C the second weight loss began and ended at about 750°C. The exothermal peak centered at 682°C implies the breakdown of Wells-Dawson anion framework and transformation and the release of most organic fragments. At temperatures higher than 800°C, even up to 900°C, there is still weight loss and the sample did not arrive at constant mass. All these facts indicate that the thermal decomposition of **2** undertook a complicated process including cracking, dehydrogenization, carbonization, and oxidation of the organic molecules in the presence of POMs.

4. Conclusion

In summary, two organic–inorganic hybrid compounds have been synthesized by hydrothermal technique and structurally characterized. Compound **1** exhibits ladder chain structure, very different from that of the reported compounds [22, 23], whereas **2** has a 3-D covalently bonded structure built from saturated Wells-Dawson tungstoarsenate polyoxoanion and copper complex with rigid and flexible ligands. This work demonstrates that the choice of reductant and pH are crucial to construct high-dimensional structure from polyoxometalate building blocks and Cu-organonitrogen complexes. Future work will focus on the synthesis of organic–inorganic hybrids based on other types of polyoxometalates and Cu-organonitrogen complexes.

Supplementary material

X-ray crystallographic files for **1** and **2** in CIF format, XPS, and TG data for compounds **1** and **2**. The CIF files have been deposited with the Cambridge Crystallographic Data Center, CCDC reference numbers: 606121 and 691125. Copies of this information may be obtained free of charge from The Director, CCDC, 12 Union Road, Cambridge, CB2 IEZ, UK (Fax: +44123336033; Email: deposit@ccdc.cam.ac.uk).

Acknowledgement

This work was supported by the Analysis and Testing Foundation of Northeast Normal University.

References

[1] M.T. Pope, A. Müller (Eds.). *Polyoxometellates: From Platonic Solids to Antiretro-viral Activity*, Kluwer, Dordrecht (1994).
[2] C.L. Hill (Guest Ed.) Special issue on polyoxometalates, Chem. Rev., 98 (1998).

[3] P. Mialane, A. Dolbecq, J. Marrot, E. Rivière, F. Sécheresse. *Chem. Eur. J.*, **11**, 1771 (2005).

[4] C.R. Mayer, C. Roch-Marchal, H. Lavanant, R. Thouvenot, N. Sellier, J.-C. Blais, F. Sécheresse. *Chem. Eur. J.*, **10**, 5517 (2004).

[5] C. Zhang, R.C. Howell, K.B. Scotland, F.G. Perez, L. Todaro, L.C. Francesconi. *Inorg. Chem.*, **43**, 7691 (2004).

[6] U. Kortz, F. Hussain, M. Reicke. *Angew. Chem. Int. Ed.*, **44**, 3773 (2005).

[7] B.S. Bassil, S. Nellutla, U. Kortz, A.C. Stowe, J . van Tol, N.S. Dalal, B. Keita, L. Nadjo. *Inorg. Chem.*, **44**, 2659 (2005).

[8] P.J. Hagrman, D. Hagrman, J. Zubieta. *Angew. Chem., Int. Ed.*, 38, 2638 (1999).

[9] M.I. Khan, E. Yohannes, D. Powell. *Chem. Commun.*, 23 (1999).

[10] V. Smith. *Chem. Rev.*, **88**, 149 (1988).

[11] T. Kresge, M.E. Leonowiez, W.J. Roth, J.C. Vartuli, J.S. Beck. *Nature*, **359**, 710 (1992).

[12] S. Mann. *Nature*, **365**, 499 (1993).

[13] P.Q. Zheng, Y.P. Ren, L.S. Long, R.B. Huang, L.S. Zheng. *Inorg. Chem.*, **44**, 1190 (2005).

[14] Y.P. Ren, X.J. Kong, X.Y. Hu, M. Sun, L.S. Long, R.B. Huang, L.S. Zheng. *Inorg. Chem.*, **45**, 4016 (2006).

[15] H.Y. An, E.B. Wang, D.R. Xiao, Y.G. Li, Z.M. Su, L. Xu. *Angew. Chem. Int. Ed.*, **45**, 904 (2006).

[16] Y. Xu, J.Q. Xu, K.L. Zhang, Y. Zhang, X.Z. You. *Chem. Commun.*, 153 (2000).

[17] W.B. Yang, C.Z. Lu, H.H. Zhuang. *J. Chem. Soc., Dalton Trans.*, 2879 (2002).

[18] G.Y. Luan, Y.G. Li, S.T. Wang, E.B. Wang, Z.B. Han, C.W. Hu, N.H. Hu, H.Q. Jia. *Dalton Trans.*, 233 (2003).

[19] (a) J.Y. Niu, Z.L. Wang, J.P. Wang. *Inorg. Chem. Commun.*, **6**, 1272 (2003); (b) J.Y. Niu, J.W. Zhao, J.P. Wang, P.T. Ma. *J. Mol. Struct.*, **699**, 85 (2004); (c) J.Y. Niu, Y. Shen, J.P. Wang. *J. Mol. Struct.*, **733**, 19 (2005).

[20] R.N. Devi, E. Burkholder, J. Zubieta. *Inorg. Chim. Acta*, **348**, 150 (2003).

[21] L. Lisnard, A. Dolbecq, P. Mialane, J. Marrot, F. Sécheresse. *Inorg. Chim. Acta*, **357**, 845 (2004).

[22] (a) X. Wang, X. Lu, P. Li, X. Pei, C. Ye. *J. Coord. Chem.*, **61**, 3753 (2008); (b) H.-B. Liu, Y. Sun, Y.-G. Chen, F.-X. Meng, D.-M. Shi. *J. Coord. Chem.*, **61**, 3102 (2008); (c) M.-X. Li, G.-L. Guo, J.-Y. Niu. *J. Coord. Chem.*, **61**, 2896 (2008); (d) J. Meng, X. Wang, Y. Ma, E. Wang, X. Xu. *J. Coord. Chem.*, **61**, 2853 (2008); (e) Y. Ding, H. Chen, E. Wang, Y. Ma, X. Wang. *J. Coord. Chem.*, **61**, 2347 (2008); (f) J. Sha, J. Peng, H. Liu, J. Chen, A. Tian, B. Dong, P. Zhang. *J. Coord. Chem.*, **61**, 1221 (2008).

[23] (a) H. Chen, Y. Ding, X. Xu, E. Wang, W. Chen, S. Chang, X. Wang. *J. Coord. Chem.*, **62**, 347 (2009); (b) J. Cao, S. Liu, Y. Ren, R. Cao, C. Gao, X. Zhao, L. Xie. *J. Coord. Chem.*, **62**, 1381 (2009); (c) J. Wang, Y. Feng, P. Ma, J. Niu. *J. Coord. Chem.*, **62**, 1895 (2009); (d) Z. Li, R. Cui, G. Xue, H. Hu, F. Fu, J. Wang. *J. Coord. Chem.*, **62**, 1951 (2009); (e) M. Wei, H. Xu, R. Sun. *J. Coord. Chem.*, **62**, 1989 (2009).

[24] Y.K. Li, Y.G. Zhou, B.B. Su, Z.H. Zhao, Z.F. Zhang. *Eur. J. Inorg. Chem.*, 5662 (2007).

[25] J.Q. Sha, C. Wang, J. Peng, J. Chen, A.X. Tian, P.P. Zhang. *Inorg. Chem. Commun.*, **10**, 1321 (2007).

[26] A.X. Tian, J. Ying, J. Peng, J.Q. Sha, Z.G. Han, J.F. Ma, Z.M. Su, N.H. Hu, H.Q. Jia. *Inorg. Chem.*, **47**, 3274 (2008).

[27] Z.M. Zhang, Y.G. Li, Y.H. Wang, Y.F. Qi, E.B. Wang. *Inorg. Chem.*, **47**, 7615 (2008).

[28] A. Teze, G. Herve. *Inorg. Synth.*, **27**, 85 (1990).

[29] R. Contant, R. Thouvenot. *Inorg. Chim. Acta*, **212**, 41 (1993).

[30] G.M. Sheldrick. *SHELXL 97, Program for Crystal Structure Refinement*, University of Göttingen, Germany (1997).

[31] D.Q. Chu, J.Q. Xu, L.M. Duan, T.G. Wang, A.Q. Tang, L. Ye. *Eur. J. Inorg. Chem.*, 1135 (2001).

[32] H. Jin, C. Qin, Y.-G. Li, E.-B. Wang. *Inorg. Chem. Commun.*, **9**, 482 (2006).

[33] M.-X. Li, J. Du, J.-P. Wang, J.-Y. Niu. *Inorg. Chem. Commun.*, **10**, 1391 (2007).

[34] J. Sha, J. Peng, H. Liu, B. Xue, J. Chen, A. Tian, B. Dong, P. Zhang. *J. Mol. Struct.*, **871**, 85 (2007).

[35] J. Sha, J. Peng, H. Liu, J. Chen, B. Dong, A. Tian, Z. Su. *Eur. J. Inorg. Chem.*, 1268 (2007).

[36] X.-J. Kong, Y.-P. Ren, P.-Q. Zheng, Y.-X. Long, L.-S. Long, R.-B. Huang, L.-S. Zheng. *Inorg. Chem.*, **45**, 10702 (2006).

[37] F.-X. Meng, Y.-G. Chen, H.-B. Liu, H.-J. Pang, D.-M. Shi, Y. Sun. *J. Mol. Struct.*, **837**, 224 (2007).

[38] Y. Wang, D. Xiao, L. Fan, E. Wang, J. Liu. *J. Mol. Struct.*, **843**, 87 (2007).

[39] A. Kibayashi, Y. Sasaki. *Bull. Chem. Soc. Jpn.*, **48**, 885 (1975).

[40] B. Dawson. *Acta Crystallogr.*, **6**, 113 (1953).

[41] R.J. Colton, J.W. Rabalais. *Inorg. Chem.*, **15**, 236 (1976).

[42] I.D. Brown, D. Altermatt. *Acta Crystallogr., Sect. B*, **41**, 244 (1985).

[43] G.A. Vernon, G. Stucky, T.A. Carlson. *Inorg. Chem.*, **15**, 278 (1976).

[44] Y.J. Jiang, Q.M. Gao. *Mater. Lett.*, **61**, 2212 (2007).